International Journal of Pressure Vessels and Piping 162 (2018) 46–51

Contents lists available at ScienceDirect

International Journal of Pressure Vessels and Piping

journal homepage: www.elsevier.com/locate/ijpvp

Post-buckling behavior of fluid-storage steel horizontal tanks

Carlos A. Burgos[a], Rossana C. Jaca[b], Luis A. Godoy[c,*]

[a] FCEFyN, Universidad Nacional de Córdoba, Córdoba, Argentina
[b] Engineering School, Universidad Nacional del Comahue, Neuquén, Argentina
[c] Institute for Advanced Studies in Engineering and Technology, IDIT UNC-CONICET, FCEFyN, Universidad Nacional de Córdoba, Córdoba, Argentina

ARTICLE INFO

Keywords:
Horizontal tanks
Buckling
Finite element analysis
Shells
Vacuum
Fluid

ABSTRACT

This paper focuses on the buckling and post-buckling of horizontal steel tanks with conical end-caps, supported on discrete saddles, under pressure caused by internal vacuum and liquid pressure. Linear bifurcation, as well as geometrically nonlinear analyses with imperfections, was performed on a single geometric configuration in order to highlight modeling differences, imperfection sensitivity, and post-buckling behavior. Results are presented for (a) increasing uniform external pressure; (b) increasing pressure under fixed fluid level; (c) coupled increasing pressure and decreasing fluid. For perfect shells, the lowest maximum loads are reached at the conical end-caps; however, imperfection-sensitivity is more stringent for the cylindrical shell than for the conical caps, with the consequence that the buckling mode has displacements in the cylinder and in the conical caps. The influence of radius to thickness ratio and fluid level are investigated by means of parametric studies.

1. Introduction

In a recent review on the structural behavior of liquid storage tanks, Zingoni [1] showed that considerable effort has been given to explore the buckling behavior of vertical tanks but only a few papers on horizontal tanks are found in the technical literature. Explanations for this lack of urgency in research may be that horizontal tanks (with a volume capacity usually limited to 200 m^3) have a much smaller storage capacity than vertical ones; their cost of fabrication are much lower; and the consequences to be expected from a structural failure are less dramatic than in a vertical tank. But safe designs are expected in all cases and research involving non-linear behavior is needed to fill the voids in our current knowledge. Failure of horizontal tanks is often found in oil facilities, such as the tank shown in Fig. 1.

The study of Chan et al. [2] for aboveground horizontal tanks under saddle supports under hydrostatic pressure was limited to the stress analysis, and stresses were compared with allowable buckling stresses as given by design recommendations. They found that the type of support (the tank may be either loose or welded to the saddle) has great importance on buckling mode: Buckling would initiate due to meridional stresses at mid-span for welded supports, whereas circumferential stresses dominate for loose supports. The dominant parameters identified in these cases were radius R, thickness t and length L of the vessel, distance between supports Ls and saddle embracing angle; the width of the support was not considered to be important in any case. Along similar lines, Banks et al. [3] performed parametric studies to evaluate maximum plastic strains.

Studies by Magnucki and Stasiewicz [4] identified critical pressures (i.e. a combination of hydrostatic pressure and internal negative pressures) and the effect of R/t ratios for horizontal tanks with elliptical end closures. A Linear Bifurcation Analysis (LBA) was performed using Donnell's equations and Galerkin Method. Magnucki et al. [5] were also interested in the optimization of the geometry (as given by L/R) for a given volume of a horizontal tank in which strength and stability were taken as design constraints.

Numerical studies were conducted by Jasion and Magnucki [6] and Jasion [7] in which buckling performance was investigated for barreled tanks, to find what improvements in buckling capacity were obtained with respect to cylindrical geometries.

Most previous studies concentrate on stress or buckling analysis as obtained from LBA. This paper focuses on the nonlinear buckling and post-buckling of horizontal tanks with conical end-closures, supported on discrete saddles, under pressures caused by internal vacuum and liquid pressure.

2. Illustrative case study

2.1. Geometry of case studied

Because of their smaller size as compared with their vertical counterparts, typical horizontal aboveground tanks are constructed using steel courses which are welded in workshops. Most common R/t ratios

* Corresponding author.
E-mail address: luis.godoy@unc.edu.ar (L.A. Godoy).

https://doi.org/10.1016/j.ijpvp.2018.03.001
Received 7 December 2017; Received in revised form 1 February 2018; Accepted 6 March 2018
Available online 10 March 2018
0308-0161/

Fig. 1. Buckled tank with three saddle supports, Peñuelas, Puerto Rico (Photograph by LAG).

range between 150 and 500, having smaller slenderness than large vertical tanks. Design of such tanks in the US follows API 12D [8] for welded-in-the-field tanks with capacities between 75 and 1500 m^3; and API 12F [9] for shop-welded tanks with volumes between 13.5 and 75 m^3. Both API 12D and 12F are oriented to tanks employed in the oil industry. For small tanks (up to 190 m^3) other features are covered by Underwriters Lab documentation [10].

Depending on the length L, tanks may be supported on two or three saddles. The schematic geometry of a horizontal tank is shown in Fig. 2 for three saddles and conical end-closures.

This three-saddle configuration is studied in this work, with diameter D = 2.4 m, length L = 5.9 m, t = 6.35 mm (1/4 in), and 25 m^3 volume, supported on equally spaced welded saddles. With reference to Fig. 2, s_3 = 2.175 m, s_2 = 0.825 m; and s_1 = 0.15 m. The conical end-closures have the same thickness as the cylinder. ASTM A36 steel is assumed in the computations, with E = 206 GPa and ν = 0.3 (Poisson).

2.2. Finite element model employed in the analysis

The structure has been investigated by means of a finite element model using ABAQUS [11]. Eight-node elements (identified as S8R5 in ABAQUS) were used in the discretization of the cylindrical part, whereas six-node triangles (STRI65) covered the apex of the conical caps. Convergence studies were performed in each case to identify an appropriate mesh of elements.

LBA was used as a first stage to obtain classical critical loads (eigenvalues) and modes (eigenvectors) of the shell, followed by Geometrically Nonlinear Analysis (GNLA) or Geometrically Nonlinear Analysis with Imperfections (GNIA) to follow the non-linear path with Riks algorithm [12] [13]. In each case, stresses were evaluated to assess the possibility of finding shell plasticity.

Fluid level was assumed to be fixed for most analysis, but parametric studies were performed to take fluid level h into account from zero fluid (h/D = 0) to full tank under fluid (h/D = 1).

Implementation of load combinations in ABAQUS requires the use of steps as follows: The load P is represented in terms of P_0, the load at the end of the previous step, and a scalar factor λ which is multiplied by the difference between P_{ref} and P_0, where P_{ref} is the load for the current step. Thus,

$$P = P_0 + \lambda(P_{ref} - P_0) \quad (1)$$

For a fixed fluid level and increasing pressure, P_0 is due to fluid and P_{ref} to pressure.

3. Buckling of empty horizontal tanks under uniform pressure

3.1. Linear bifurcation analysis (LBA)

For an empty tank with increasing external pressure, LBA provided a critical pressure of 68.8 kPa, with a bifurcation buckling mode affecting the conical caps and not the cylindrical part of the tank (see Fig. 3). The first mode for which the cylinder buckles is mode 17, at a pressure of 93.9 kPa. As a reference value, the classical buckling load (LBA) for a cylindrical shell having the same length but without saddle supports is 85.4 kPa. The sequence of eigenvalues and associated eigenmodes predicted by LBA is largely dependent on the shell configuration, i.e. geometric details of the conical caps.

This first analysis cannot be taken to draw final conclusions even for this particular case, because it is based on linearized analysis and does not take into account effects of nonlinearity and imperfection sensitivity. Thus, the influence of imperfections is reported in the following sections.

3.2. Geometrically nonlinear analysis with imperfections (GNIA)

Results for an empty tank using GNIA are shown in Fig. 4, as computed using Riks algorithm in ABAQUS. The figure shows the scalar λ parameter used to increase the load versus the displacement at a characteristic point of the shell (point A in Fig. 4). Although the choice of the point at which displacements are plotted may improve visualization of the results, the load levels at which instability occurs would be detected at any point having non-zero displacements. In each case, identification of what part of the tank buckles (either the cylindrical part or the end caps) has been based on observation of the buckling mode computed from the nonlinear analysis.

As expected, the equilibrium path for the perfect case (identified by ξ = 0 in Fig. 4) has an almost linear behavior up to a maximum load level, at which limit point buckling is identified in the path. This maximum occurs at a load level which is lower than the LBA critical load.

Imperfection-sensitivity has been next investigated by introduction geometric deviations with a specified shape and a maximum amplitude of deviation denoted by the scalar ξ. The geometrically nonlinear analysis with geometric imperfections was performed under an assumed initial geometry which deviates from the perfect cylindrical shape. Following the original work of Koiter [14], Thompson and Hunt [15] and others, we assumed an imperfection with the shape of an eigenmode. In this case we explored the influence of two such

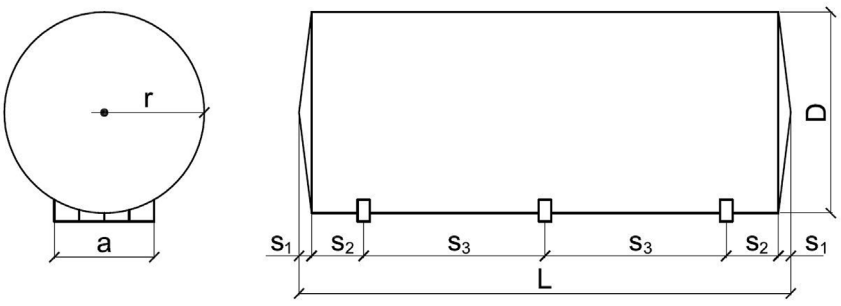

Fig. 2. Geometry of the horizontal tank investigated in this paper as case-study.

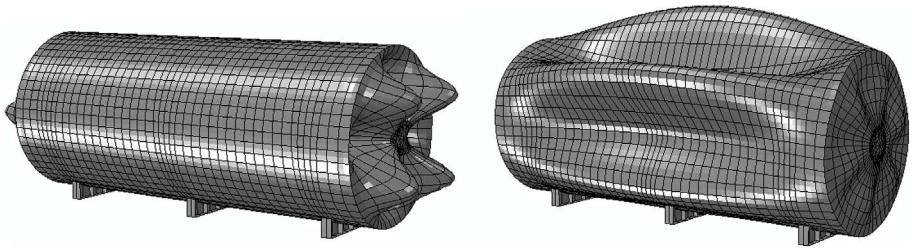

Fig. 3. Eigenmodes 1 and 17 computed from LBA study. Eigenmode 1 affects just the conical shell, whereas eigenmode 17 mainly affects the cylindrical shell.

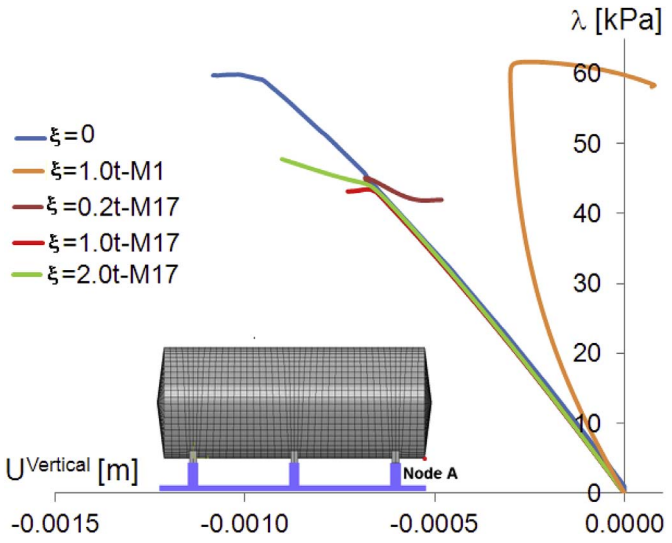

Fig. 4. Equilibrium paths for a tank under uniform external pressure, computed with GNIA, having imperfections with the shape of Mode 1 and Mode 17 (Node A).

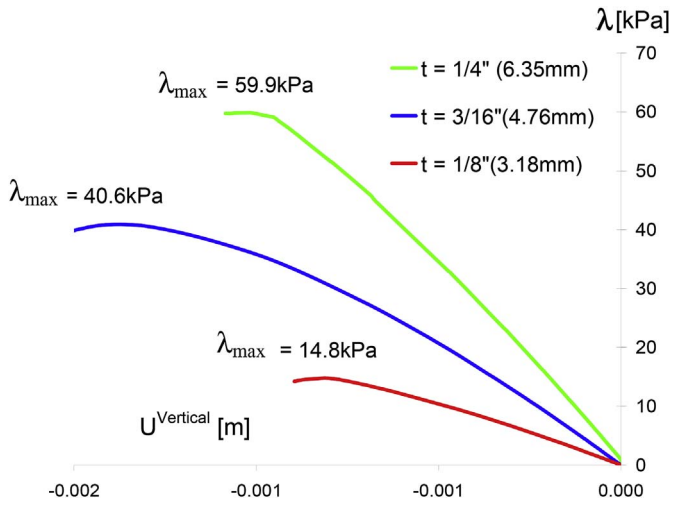

Fig. 5. Influence of shell thickness on buckling under uniform pressure, using GNLA (ξ = 0). Displacement measured at point A in Fig. 4.

eigenmodes, i.e. the first one, affecting the conical shell, and mode 17, affecting the cylindrical body. In both cases, increasing amplitudes in the range $0.2 < \xi/t < 2$ were used to investigate imperfection-sensitivity.

An imperfection with the shape of Mode 1 (just affecting the conical caps) modifies the equilibrium path but the maximum load that can be reached remains unchanged with respect to the perfect shell case. This is shown in Fig. 4 for ξ = t. On the other hand, the nonlinear problem is highly sensitive to imperfections affecting the cylinder, such as Mode 17, which causes a reduction in load bearing capacity from above 59.9 kPa–43.5 kPa for ξ = t, thus indicating a drop of about 25%. The postbuckling equilibrium path is unstable. For higher imperfection amplitudes, say ξ = 2t, the path does not show a maximum and the behavior ceases to be dominated by buckling.

In conclusion, LBA predicts modes affecting the conical caps, but GNIA predicts cylinder modes at lower pressure levels, even for imperfection amplitudes of the order of the shell thickness.

3.3. Influence of shell thickness

The studies described in the previous sections were presented with reference to a shell having thickness t = 6.35 mm (¼"), but the buckling process is highly dependent on shell thickness. To investigate the incidence of t, cases with t = 4.76 mm (3/16″) and t = 3.18 mm (1/8″) are considered in this section to account for commercially available plate thicknesses.

Results under uniform pressure are shown in Fig. 5, in which the maximum in load bearing capacity reduces from almost 60 KPa for 6.35 mm to 40.9 kPa for 4.76 mm, and to 14.8 kPa for 3.18 mm.

This is a nonlinear relation between limit point load and shell thickness.

4. Buckling of horizontal tanks having fixed fluid and increasing pressure

This analysis was performed in two steps: First, under self-weight and fluid level, a second under gradually increasing pressure. The equilibrium path was computed by Riks algorithm and results for a perfect geometry are reported in this section. Because loads are initially applied to the structure before pressure, the second step was computed on a deflected configuration.

Results are shown in Fig. 6 for values of λ for various fluid levels h, and for a geometrically perfect initial configuration ξ = 0.

The effect of the pre-load in this case operates in a way similar to an initial deviation from the geometrically perfect shell, because there are initial displacements before external pressure is applied. As a

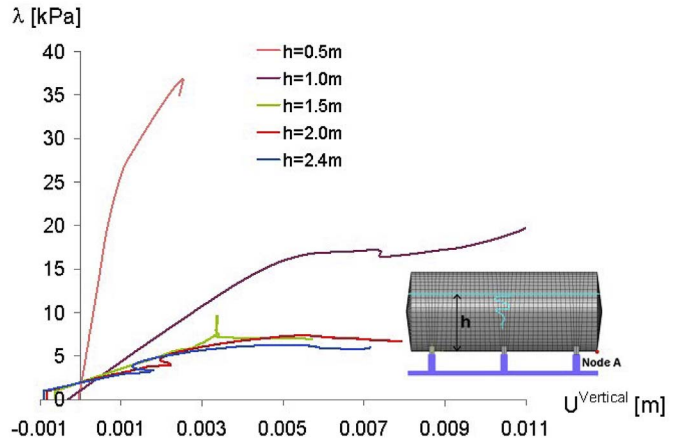

Fig. 6. Nonlinear equilibrium paths for horizontal tank under various fluid levels using GNLA, R/t = 189. Displacement measured at point A in Fig. 4.

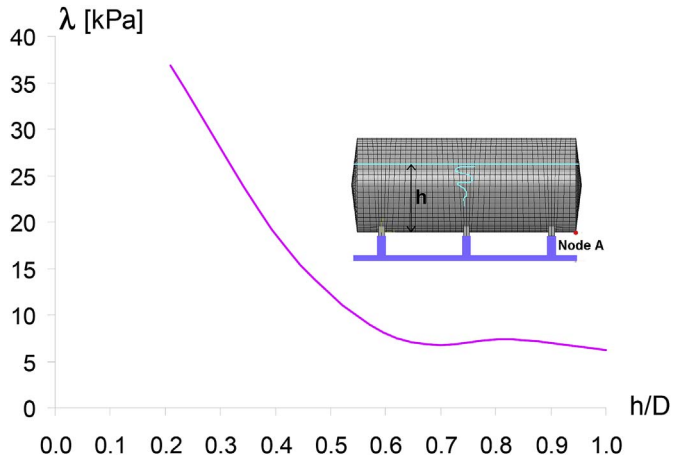

Fig. 7. Sensitivity of load factor λ to initial fluid level h/D, data as in Fig. 6.

consequence of that, the maximum load factor λ that the system can reach decreases with increasing h.

A plot of λ versus h/D shown in Fig. 7 takes a form similar to an imperfection-sensitivity plot: Small values of h/D cause a large drop in λ, whereas larger values of h/D are only responsible for small further reduction in λ.

The deflected shape of the tank is shown in Fig. 8 for a configuration with initial fluid h/D = 1. Compression develops on the entire shell at the top of the tank, at mid-height, and at the lower part where saddles are located. Notice that this mode involves displacements in both the cylinder and the end caps.

5. Tanks with decreasing fluid and increasing pressure

Results presented in the last section are rather simplified in the sense that the fluid is set to a fixed level and pressures act on the complete tank. However, the process of decreasing fluid is more complex because the effect of pumping fluid out of the tank decreases its level and increases pressures; both effects are part of the same process.

5.1. Geometrically nonlinear analysis (GNLA)

Another way to view this problem is to consider that the tank has a fluid level at the beginning of the operation, which is gradually decreased by the use of a pump, which in turn causes vacuum. Fluid flow occurs until the tank is emptied, after which only vacuum remains active. Three stages are needed to model this process using ABAQUS: First, computation of initial effects due to self-weight and fluid level; second, simultaneous inclusion of vacuum and a load that counteracts the hydrostatic pressure. This step requires identification of when fluid action is cancelled. Third, only pressure acts on the tank.

To illustrate the process, consider the case with h/D = 1, i.e. the tank is full and operations are applied to empty the tank causing

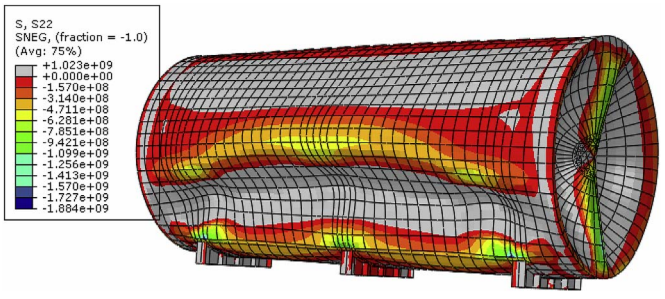

Fig. 8. Circumferential stresses (compression) on deflected shape of tank for h = 2.4 m (GNLA).

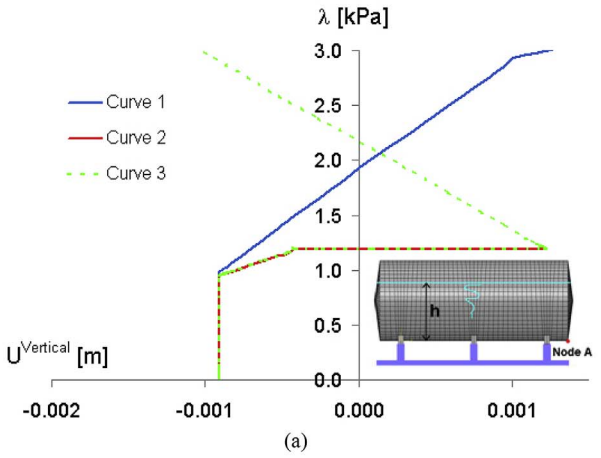

(a)

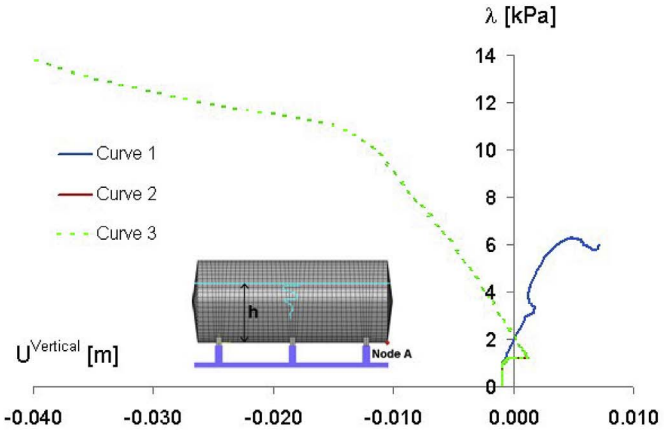

(b)

Fig. 9. Equilibrium path for decreasing fluid and increasing pressure. (a) Details at the early stages of the process; (b) Advanced post-critical states (Node A).

vacuum.

Results of the early stages are shown in Fig. 9(a), whereas advanced states are shown in Fig. 9(b). Notice that the path in Fig. 8(b) increases monotonically with pressure, reaching high levels of deformation.

Curve 1 in Fig. 9(a) and (b), is drawn for vacuum in a tank with h/D = 1, which is similar to the early stages shown in Fig. 4. Point A at the junction between cylinder and conical cap has a downwards displacement due to the fluid stored. As vacuum is applied the point in the shell moves upwards due to the applied suction.

Curve 2 starts at the same initial level with negative displacement, but the response changes because simultaneously with the application of vacuum there is a decrease in fluid level. At the end of this stage, there is no remaining fluid in the tank. There are upwards displacements but with a path which is different from that in Curve 1. Curve 3 is a continuation of the path in Curve 2, caused by the application of vacuum on a deflected structure from the state at the end of Curve 2. There is a change in the response with downwards displacements in a monotonically increasing path.

Notice that the initial deflected shape act as an initial imperfection in the structure, on which vacuum is applied: This induces a different mode to what would be obtained if vacuum is applied on the perfect structure or with imperfections following LBA eigenvectors.

The incidence of fluid level at the onset of the process is shown in Fig. 10, for h/D = 0.42; 0.83; and 1 with h = 1.0 m, 2.0 m and 3.0 m respectively. For the case with lower initial fluid level (h/D = 0.42), there is a maximum in the load path at λ = 27.65 kPa, but this maximum is not visualized for higher fluid levels.

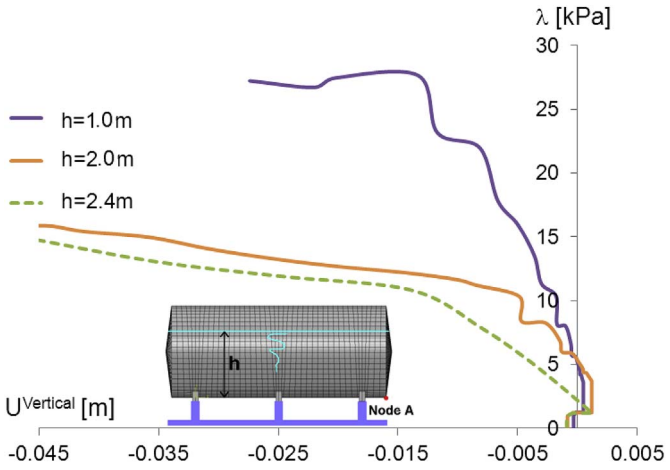

Fig. 10. Equilibrium paths for fluid discharge starting from various levels and variable internal vacuum (Node A).

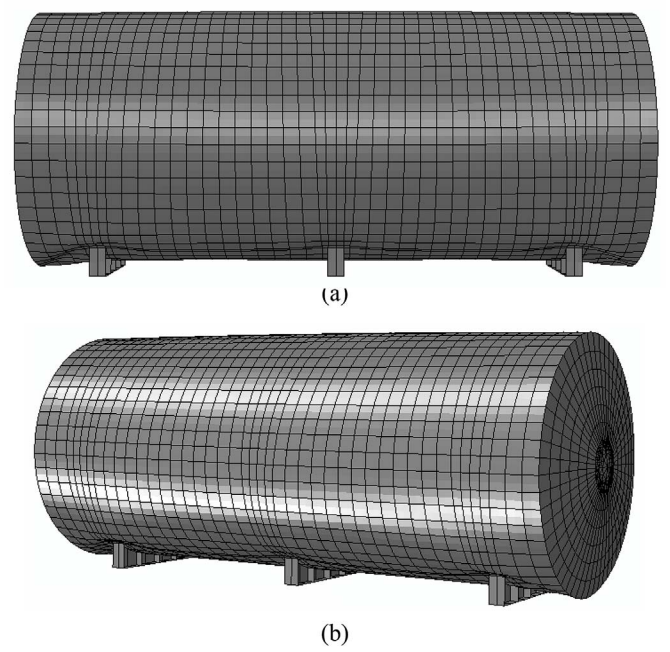

Fig. 11. Deflected shape of tank for h = 2.0 m, (λ = 16.45 kPa), (a) Side view, (b) Rotated view.

The deflected shape of the tank with an initial fluid level h/D = 0.83 is shown in Fig. 11. The vertical displacement at A is 50 mm for λ = 16.45 kPa. If the initial fluid level was reduced to h/D = 0.42, the vertical displacement reduces to 13 mm for λ^{max} = 27.65 kPa, and to U_A^{vert} = 53 mm for an advanced post-critical state with λ = 34.74 kPa. The buckling mode in these cases is similar to what was shown in the photograph of Fig. 1 for a collapsed tank.

It was assumed that the material remains elastic in all previous considerations. However, this can only be ascertained from a study of von Mises stresses in the tank. For h/D = 0.83 the deflected shape is given in Fig. 12. Assuming yield stress σ_y = 216 MPa the shell remains elastic at all points up to a load level of λ = 2.58 kPa, but localized yielding occurs at the saddles for higher load levels. The existence of localized stresses at the junctions between shell components has been addressed by several authors (see, for example, the work of Zingoni [16] for cone-cone junctions); this may be seen to occur in the results of Fig. 12, although in the present case the stresses associated with the geometric discontinuity are less severe than those at the saddle supports.

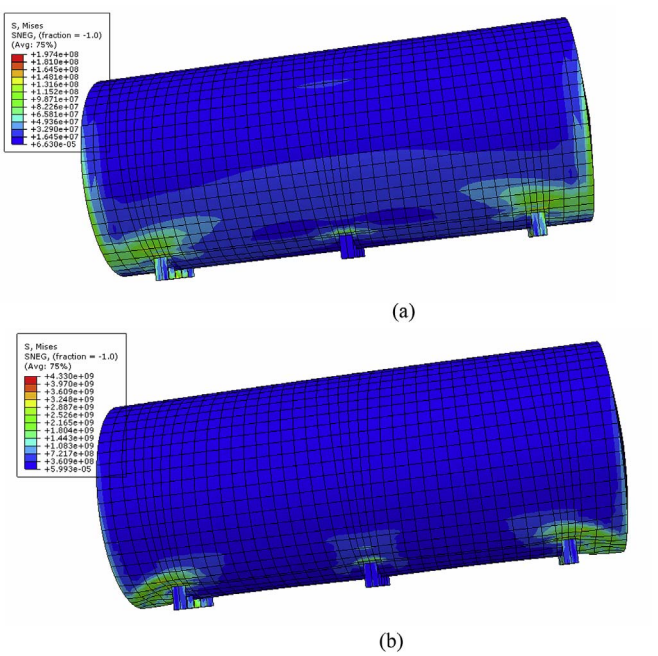

Fig. 12. Von Mises equivalent stresses. (a) For λ = 2.58 kPa, elastic behavior, (b) For λ = 11.65 kPa, yielding at saddle supports.

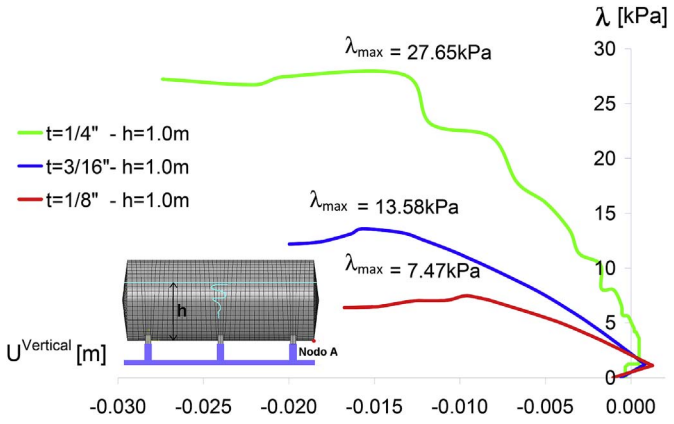

Fig. 13. Influence of shell thickness on buckling under fluid discharge plus vacuum, h/D = 0.42.

5.2. Influence of shell thickness

The influence of decreasing shell thickness t on the more complex process of simultaneous reduction of fluid and increasing vacuum is shown in Fig. 13, again for three values of t.

Maximum values of λ that are reached decrease with decreasing t, and the effect is more severe than under the sole action of pressure (Fig. 5). For example, for t = 6.35 mm and h/D = 0.42, there is 46% reduction in vacuum pressure with respect to the condition of tank without fluid.

6. Conclusions

The buckling and post-buckling of horizontal fluid-storage tanks has been investigated in this work by means of bifurcation (LBA) and nonlinear (GNIA, GNLA) analyses. Based on the results reported for a single case investigated in detail, some conclusions may be drawn as follows:

- An LBA may yield misleading results in this problem, even for the

uniform pressure load case. For the considered tank, the lowest eigenvalue via LBA was identified for a mode affecting the conical caps, with a cylinder eigenvalue occurring at a higher load. However, a GNIA study showed that if an imperfect geometry is taken into account, the lowest loads are detected for cylinder modes, in which case there is 25% drop with respect to the perfect case. Thus, one should expect the shell to buckle with displacements in the cylinder.

- For fixed fluid level and increasing pressure, further reductions are computed with GNLA with respect to values with GNIA. For example, for initial fluid level h/D = 0.42, a maximum is reached at less than half the critical load under uniform pressure.
- Unlike the behavior of vertical tanks, in which a fluid plays a stabilizing effect on buckling [17], in a horizontal tank the fluid has the opposite effect. This reduction in load bearing capacity is associated with the stresses at the top of the tank caused by the presence of the fluid, thus adding further compressions.
- The shell thickness plays a crucial role in buckling: Under uniform pressure, an increase of 33% in the R/t ratio causes a similar reduction in critical load. The same increase in R/t is accompanied by 100% reduction in maximum load for the process of decreasing fluid and increasing pressure.
- Only a case study with a given geometry has been performed in this work to highlight the differences between various modeling approaches. The authors have not attempted to address parametric studies covering geometric details of the tank itself. This is seen as a topic for further research, aiming to provide design recommendations.

Acknowledgements

The authors thank the support given to this research from grants of the National University of Comahue, SECYT-National University of Cordoba, CONICET-PIP Grant 00126/2013, and CONICET-UE Grant titled “Vulnerability of infrastructure and physical environment associated with fuel transportation and storage”.

References

[1] A. Zingoni, Liquid containment shells of revolution: a review of recent studies on strength, stability and dynamics, Thin-Walled Struct 87 (2015) 102–114.
[2] G.C.M. Chan, A.S. Tooth, J. Spence, A study of the buckling behaviour of horizontal saddle supported tanks, Thin-Walled Struct 30 (1–4) (1998) 3–22.
[3] W.M. Banks, D.H. Nash, A.E. Flaherty, W.C. Fok, A.S. Tooth, A simplified design approach to determine the maximum strains in a GRP vessel supported on twin saddles, Int J Pres Ves Pip 77 (2000) 837–842.
[4] K. Magnucki, Stasiewicz, Critical sizes of ground and underground horizontal cylindrical tanks, Thin-Walled Struct 41 (2003) 317–327.
[5] K. Magnucki, J. Lewinski, P. Stasiewicz, Optimal sizes of a ground-based horizontal cylindrical tank under strength and stability constraints, Int J Pres Ves Pip 81 (2004) 913–917.
[6] P. Jasion, K. Magnucki, Elastic buckling of barreled shell under external pressure, Thin-Walled Struct 45 (2007) 393–399.
[7] P. Jasion, Stability analysis of a liquid filled barreled horizontal tank, Proc Appl Math Mech 8 (2008) 10291–10292.
[8] API Standard 12D, Specification for field welded tanks for storage of production liquids, American Petroleum Institute, Washington, D.C, 1994.
[9] API Standard 12F, Specification for shop welded tanks for storage of production liquids, American Petroleum Institute, Washington, D.C, 1994.
[10] Underwriters Laboratories, Standard UL-142, Steel aboveground tanks for flammable and combustible liquids, Underwriters Laboratories Inc., Northbrook, Illinois, 1998.
[11] ABAQUS, User's manuals, version 6.3, Hibbitt, Karlsson and Sorensen, Inc, Rhode Island, 2006.
[12] E. Riks, The application of Newton's method to the problem of elastic stability, J Appl Mech 39 (1972) 1060–1065.
[13] E. Riks, An incremental approach to the solution of snapping and buckling problems, Int J Solid Struct 15 (1979) 529–551.
[14] A.M.A. van der Heijden (Ed.), W. T. Koiter's elastic stability of solids and structures, Cambridge University Press, Cambridge, UK, 2012.
[15] J.M.T. Thompson, G.W. Hunt, A general theory of elastic stability, Wiley, London, 1973.
[16] A. Zingoni, Discontinuity effects at cone-cone axisymmetric shell junctions, Thin-Walled Struct 40 (10) (2002) 877–891.
[17] L.A. Godoy, Buckling of vertical oil storage steel tanks: review of static buckling studies, Thin-Walled Struct 103 (2016) 1–21.